


Evaluation of Radiation Treatment Planning Algorithms in IMRT and VMAT: A Comparative Dosimetric Study in Lung Equivalent Heterogeneous Medium

Atul Mishra (PhD Candidate)^{1,2,3*}, Ramji Pathak (PhD)^{1,2,4}, Teerth Raj Verma (PhD)⁵, Anoop Kumar Srivastava (PhD)⁶, Surendra Prasad Mishra (PhD)⁶, Kailash Kumar Mittal (MD)³, Sudesh Kumar Singh (PhD)^{1,2}

ABSTRACT

Background: In Radiotherapy, computation of dose is important since in a small field with heterogeneity, dose is usually computed with discrepancies.

Objective: The present study was aimed to evaluate the dosimetry of treatment planning algorithms in lung equivalent heterogeneous medium for Volumetric Modulated Arc Therapy (VMAT) with step and shoot Intensity-Modulated Radiation Therapy (ss-IMRT), and dynamic Intensity-Modulated Radiation Therapy (d-IMRT).

Material and Methods: In this experimental study, Computerized Imaging Reference System (CIRS) phantom was used with an inhomogeneous Racemosa wood cylinder for two types of tumors, namely, Left Lung Central Tumor (LCT) and Left Lung Peripheral Tumor (LPT) in the CIRS left lung cavity. The computed tomography (CT) datasets were employed with the generation of VMAT, d-IMRT and ss-IMRT plans for the LCT and LPT irradiated with 6 MV photon beams. In this study, the accuracy and efficacy of two algorithms: Monte Carlo (MC) and the Pencil Beam (PB), from the Monaco treatment planning system (TPS), were tested by using Gafchromic EBT3 films and CIRS thorax phantom.

Results: Regardless of treatment techniques, both algorithms exhibited higher divergence in LPT than LCT. In both LCT and LPT, the highest deviation was near the tumor-lung junction. However, the deviation was higher in the PB algorithm than MC algorithm, with a minimally acceptable variation of -0.8%.

Conclusion: The MC algorithm shows more consistency for EBT3 measured dose in lung equivalent heterogeneous medium. However, accurate dose predictions are complicated due to electronic disequilibrium within and at the interface of inhomogeneity. These constraints may cause variations from the anticipated outcomes of the treatments.

Citation: Mishra A, Pathak R, Raj Verma T, Srivastava AK, Prasad Mishra S, Mittal KK, Singh SK. Evaluation of Radiation Treatment Planning Algorithms in IMRT and VMAT: A Comparative Dosimetric Study in Lung Equivalent Heterogeneous Medium. *J Biomed Phys Eng.* 2023;13(6):503-514. doi: 10.31661/jbpe.v0i0.2206-1508.

Keywords

Radiotherapy; Algorithms; Gafchromic Film; Computed Tomography; Monte Carlo; Lung

Introduction

The improved accuracy of advanced radiation treatments has led the radiation beams to match with the size and shape of a patient's tumor almost anywhere in the body. Moreover, radiation dosim-

¹Department of Physics, Tilak Dhari P. G. College, Jaunpur, (U.P.) - 222002, India

²V.B.S. Purvanchal University, Jaunpur, (U.P.) - 222003, India

³Department of Radiation Oncology, Uttar Pradesh University of Medical Sciences, Saifai, Etawah (U.P.) - 206130, India

⁴Department of Physics, D.A.V. Degree College, Lucknow, (U.P.) - 226004, India

⁵Department of Radiotherapy, King George Medical University, Lucknow (U.P.) - 226003, India

⁶Department of Radiation Oncology, Dr. Ram Manohar Lohia Institute of Medical Sciences, Lucknow (U.P.) 226010, India

*Corresponding author: Atul Mishra
Department of Physics, Tilak Dhari P. G. College, Jaunpur, (U.P.) - 222002, India
E-mail: meetatulmishra@gmail.com

Received: 20 June 2022
Accepted: 5 November 2022

etry due to inhomogeneity remains a major concern, and the disruption of electronic equilibrium and inhomogeneity affect the intensity of photon beam and scattering properties. The lung in the thoracic cavity is one of the most heterogeneous organs, with considerable movement due to inter/intra segmental motion generated by respiratory motion, which is a possible source of failure from the intended volume irradiation. Adding a low-density inhomogeneous environment, such as the lungs, can create a 30% dose deviation [1, 2]. Various treatment planning systems (TPS) are currently performed with different algorithms to generate radiotherapy treatment plans depending on their efficacy [3, 4]. In radiotherapy, an exact dose should be delivered to targets with an effectiveness depending on the precision of the absorbed dose in the target volume and the prescribed dose. If the absorbed dose is less than the specified dose, cancer cells may become resistant to radiation or the tumor may reappear. On the other hand, if the absorbed dose is higher than the specified dose, it can result in death or major harm to normal tissues [5, 6].

The dose distribution is much more complex in the region of heterogeneous tissues, particularly in small fields and the size of the discrepancy escalates [5, 7]. A low-density medium, such as the lung in a small field usually leads to challengingly estimating dose. As a result, the selection of the treatment planning algorithms for the estimation of dose in small fields in low-density medium and a detector verifying the planned dose is important for the intended outcome [8]. Electronic Portal Dosimetry (EPID), Thermo Luminescence Dosimeter (TLD), MOSFET, Ionization Chamber Systems, and Gafchromic film are some of the methods to evaluate the estimated dose distribution [9]. The Gafchromic EBT3 film is one of the most suitable detectors for dosimetry of smaller fields with a low-density medium due to its energy independent, broad range dose-response, independence to devel-

opers, and ability to manage in-room light. After exposure, Gafchromic film does not require any chemical, physical, or thermal preparation [10, 11]. The dose estimation accuracy can only be improved if TPS employs high-quality algorithms that include multisource modelling to monitor each secondary scattered photon and electron and its subsequent dose deposition in non-equilibrium conditions [12-15].

In this study, we compared the tumor isocenter dose, dose at different points, 2D Gamma values measured by Gafchromic films in the tumor isocenter plane of lung equivalent heterogeneous medium as well as within the tumor created inside it which was irradiated with different algorithms for different treatment techniques. CIRS Lung phantom was introduced with one tumor at the center of left lung and another tumor at the periphery of left lung sharing its one end with chest mimicking Lung-Tissue interface. Thus, different algorithms based on different techniques were evaluated by comparing TPS planned data with data derived from the film-measured data.

Material and Methods

CIRS 3D phantom and Wood slabs

In this experimental study, the dynamic thorax phantom (CIRS model 008A; Computerized Imaging Reference Systems Inc., Norfolk, VA, USA) was used to investigate the dosimetry methodology in sophisticated radiation-therapeutic interventions, such as Intensity Modulated Radiation Therapy (IMRT), and Volumetric Modulated arc Therapy (VMAT). Both lungs (right and left) with Hounsfield Unit (HU) -700 were included in the Computerized Imaging Reference System (CIRS) phantom that simulates a human thorax in a medical environment. A hollow cavity (cylindrical) for the entire thorax in the left lung is provided, which could hold various and beneficial inserts for a variety of dose test instruments. In this study, two types of inserts were used: 1) lung inserts, which are made of a

cylindrical rod with the same density and material as the two lung structures and 2) a bespoke wood cylinder constructed of Ficus racemosa wood slabs (commonly recognized as Goolar in India) [Figure 1a and b].

A suitable material with the same lung density was used as a lung insert to assess the influence of heterogeneity on the radiation beam while traversing the various density materials. The use of handmade wood slabs (Ficus racemosa wood slabs) was used to mimic the inhomogeneity found in real human lungs. An empty space-like wood slab cylindrical (insert) of the same dimension (radius 3.7 cm) was employed, made of wood slabs of variable widths with about the same thickness (along the middle line) to simulate lung equivalent inhomogeneity. The wood cylinder was inserted into the hollow space provided in the thorax phantom [Figure 1b (I) and (II)].

Dosimetry Films

Gafchromic EBT[®]3 films were employed as detectors, and evaluated by the Verisoft com-

puter software Version 4.2.1 from PTW, Freiburg, Germany. While scanning the films, flat-bed scanners (EPSON A3 Transparency Unit Model: EU-88, Japan) using 200 dpi spatial resolution oriented in landscape orientation were used with the transparent mode [10, 11]. Both the scanner and the films were calibrated according to standard protocol. Films were typically cut in landscape layout and labelled for scan assessment.

Delineation of the target volume and the organs at risk

Organ images and tumor volumes were generated by 3D computed tomography, including the tissue details in Computed Tomography (CT) numbers. The CT images were used with a slice thickness of 1.5 mm using a helical 16-slice scanner (Somatom Sensation, Siemens, Germany) for actual patients. Gross Tumor Volume (GTV) contouring was done using Monaco SIM for tumor 0.5 cm uniform margins were added to the GTV to delineate the Planning Target Volume (PTV). The organ

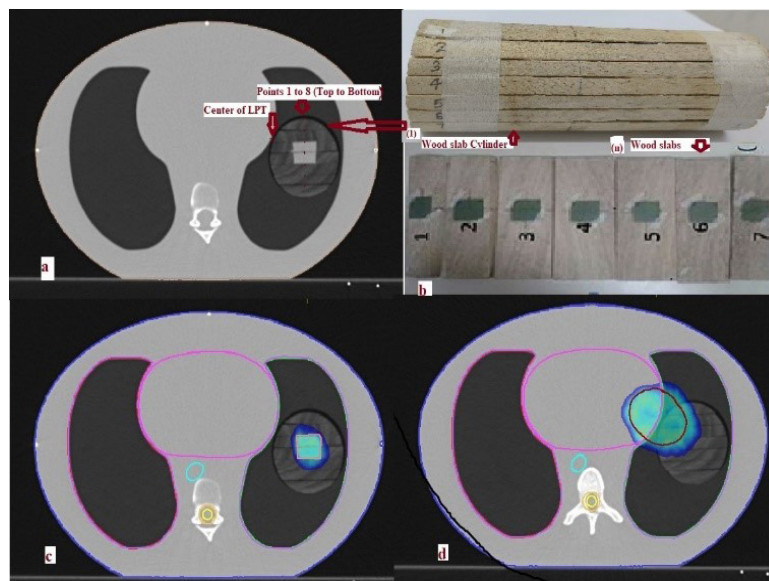


Figure 1: (a) central axis point 1 to point 8 for Left Lung Central Tumor and center of Left Lung Peripheral Tumor (LPT), (b) (I) wood slab cylinder for the cavity of computerized imaging reference systems Thorax phantom, (II) seven wood slabs with Gafchromic film for dose measurements inside the wood cylinder in total of eight surfaces, (c) location of left lung central tumor (LCT), and (d) location of Left Lung peripheral Tumor (LPT).

at risk (OAR), such as total lung and heart and spinal cord (SC) was delineated on Monaco (Version: 5.11.03) contouring workstation. Planning risk volume (PRV) was created (5 mm uniform margin to SC).

Planning with TPS

The Monaco sim system transferred contoured CT images to the Monaco planning (Elekta Medical Systems, Version: 5.11.03, Crawly, UK) workstation. The various types of plans with different algorithms were generated prior to accepting for implementation on the high energy Medical linear accelerator (Infinity; Elekta Medical Systems, Crawly, UK) with 6 MV photons and which is equipped with Multi Leaf Collimator (MLC) and Cone beam CT (CBCT) and 6D controlled couch. With a prescribed dose of 50.4 Gy, the fractionation scheme was 1.8 Gy per fraction, and all of the plans were 28 fractions. For OAR planning, the dose parameters were $V_{20} < 20\%$, $V_{30} < 12\%$, and a mean dose of < 20 Gy for the heart and both lungs. The dose threshold for the spinal cord was fixed at 45 Gy. CBCT or portal images were acquired and matched into reference images to check the accuracy of orientation. After position verification, different plans were generated, and the dose for each plan was evaluated using Gafchromic films inserted in the CIRS 3D phantom (tissue volume). On TPS, these measured dose values might well be compared to dose values planned. The dose measured and TPS data was compared to determine the efficacy of the ideally appropriate algorithm for heterogeneous environments. The investigation would find a correlation between the doses planned and received by the medium. The Monte Carlo Algorithm (MCA) and Pencil Beam Algorithm (PBA), which could perform IMRT and VMAT, were utilized for the treatment plans.

VMAT Planning

Each VMAT plan was designed with dual arcs (2A) with a start-stop angle of 180-180

degrees (30-degree arc) delivered anticlockwise with 0-180 degrees (30-degree arc) delivered clockwise to ensure whether PTV was covered by at least 95% of the prescribed dose. All plans were developed with the Monaco TPS, which used a changing dose rate with the gantry's increment angle at 30 degrees. All contouring structures were sent to the TPS (Monaco). The treatment delivery strategy to generate the treatment plan was dynamic conformal arcs. In the present study, the photon beam energy was 6 MV. Sequential factors, 200 control points per arc, 0.50 cm minimal segmentation width, and medium fluence smoothing were used to optimize all plans. The parameters were computed at 0.3 cm grid spacing and 1.0 percent statistical deviation. PBA and MCA were used to optimize the designs, and the dose was determined in the target volume.

IMRT (dynamic-IMRT and step and shoot-IMRT) Planning

All IMRT plans were designed with a minimum of 95 percent of the therapeutic dose in the PTV volume. The d-IMRT plans were designed using a 500 Monitor Unit (MU)/min fixed-dose rate to obtain improved PTV coverage and lower OAR dose. Seven coplanar beams with gantry angles of 0° , 25° , 50° , 75° , 100° , 125° , and 150° and 7 Fields (7F) were used to create the plans in dynamic window mode. Plans were optimized using the sequencing parameter, with a maximum of 30 control points per beam, a minimum of 0.50 cm segment width, and fluence smoothing set to medium. The parameter grid spacing was set at 0.3 cm for the calculation, and statistical uncertainty was set to 1.0 percent. The MLC sequences were accomplished by the step and shoot window IMRT method of delivery with seven coplanar beams for ss-IMRT. The appropriate sequencing criteria were used to optimize the plans: minimal segment area 2.0 cm^2 , minimum segment width 0.50 cm and MU per segment 4.0, maximum segments per

plan 250, and fluence smoothing to medium. The remaining parameters were identical to those in d-IMRT planning. All VMAT and IMRT designs used the same isocenter and objective characteristics for normal tissue.

Experimental Setup

The experimental setup is shown in Figure 1a and b. A cavity of 8.164 cc was constructed in two successive slabs of racemosa wood cylinder. Denture relining material (density -1 g/cm³) was used to fill these two cavities [Figure 1c], referred to as Left Lung Central Tumor (LCT), and this material was also utilized in the creation of dentures. A racemosa wood cylinder containing a tumor was put within the phantom cavity with the tumor's center aligned with the central beam. The tumor was scanned on a CIRS thorax phantom with a wood cylinder at a depth of 6.5 cm (anteriorly). Another spherical tumor (37.799 cc) was formed in the periphery of the left lung, with one end touching chest tissue and imitating the lung-tissue interface, referred to as LPT (Figure 1d). Tumors were also constructed so that Gafchromic films were used to precisely measure the central plane of the tumor. For LCT, films were arranged along with the coronal section of the racemosa wood cylinder, aligned to the radiation direction with a gantry angle of zero degrees. In between the interior surface of the CIRS phantom and the racemosa wood cylinder, films were placed for LPT. The CIRS 3D Lung phantom with LCT and LPT tumor was positioned on the couch of the Infinity Linear Accelerator (with MLC 40 pairs of 1.0 cm width at isocenter) for film irradiated as per the algorithm-generated plans. Cone Beam CT (CBCT) with kilo-voltage X-ray Volumetric Imaging (XVI) match was captured for the phantom after inserting the films to replicate and verify the isocenter in the center of the tumor as planned. For irradiating the phantom's respective tumors (LCT and LPT), plans of three methods (ss-IMRT, d-IMRT, and VMAT) were prepared for a 6 MV

photon beam using both algorithms (PBA or MCA). In both situations, Gafchromic EBT-3 films were cut and marked for directions at the edge before directly positioned in the middle of the tumor plane, sharing the lung equivalent slices, causing film to incorporate dose information for the isocentric plane. One additional film strip (aside from the isocentric plane film) was held at a plane 3.5 cm from the tumor center for each plane irradiation to verify the algorithm's accuracy in estimating normal lung dose. TPS transfers the isocentric plane of each plan to Verisoft software for evaluation with the film irradiated in the same arrangement. For assessment, the resolution and grid size for both the TPS image plane and the film were maintained the same for each case.

Calculation and Comparison

The film, held at the isocentre plane and radiated, was matched with a TPS film of the same dosage plane and synced to evaluate the outcomes. The 2D gamma passing rate percentage with two delta dose and delta distance criteria of 2% and 2 mm, 3% and 3 mm, and 5% and 5 mm were used to evaluate the general matching of the measured and algorithm computed dosage planes. The final 5% and 5-mm test was used to verify the efficacy of the algorithm under adverse scenarios. The central axis absolute dose from point 1 to 8 was also compared as shown in Figure 1a. The difference in dose concerning was visually represented along that axis. Another film irradiated at a distance of 3.5 cm from the isocenter was used to compare the TPS computed dose for 2D gamma passing index using delta dose and distance criteria of 3% and 3 mm. The following relationship (Equation 1) was used to compute the percentage variation between the absolute point dose planned on TPS and the measured dose separately for MCA and PBA [8], as follows:

$$PV = \left\{ \frac{[TPSPD(MCA \text{ or } PBA) - \text{Measured Dose (Film)}]}{\text{Measured Dose (Film)}} \right\} \times 100 \quad (1)$$

where PV defines percentage variation; TP-

SPD, TPS Planned Dose; MCA, Monte Carlo Algorithm and PBA, Pencil Beam Algorithm for equation 1.

Results

Left Lung Central Tumor

Table 1 illustrates dose variation utilizing Gafchromic film and dose calculation algorithms (PBA and MCA) for LCT. In percentage, the absolute dose along the central axis (Point 4) variations from the measured dose for the cavity 8.164 cc target LCT estimated with PBA algorithm treatment plans of ss-IMRT, d-IMRT, and VMAT target outcomes were +11.6%, +10.5%, and +10.2%, respectively. For the central axis dose variations recorded for an LCT computed using MCA treatment plans of ss-IMRT, d-IMRT, and VMAT target was -1.4%, -0.9%, and -0.8%, respectively. In this study, the (+) and (-) symbol represents overestimation and underestimation, respectively. In percentage, the absolute dose along the central axis (Point 1) variations from measured estimation with PB algorithm plans of

ss-IMRT, d-IMRT, and VMAT target outcomes were +12.9%, +12.5%, and +12.5%, respectively.

Similarly, for the central axis dose, variations of -2.1%, -1.6%, and -1.2% were recorded for an LCT computed using MCA treatment plans of ss-IMRT, d-IMRT, and VMAT target, respectively. In percentage, the absolute dose along the central axis (Point 8) variations was measured using the PB algorithm generated plans of ss-IMRT, d-IMRT, and VMAT target outcomes were +11.9%, +11.5%, and +11.6%, respectively. Same for the central axis, dose variations recorded for an LCT computed using MCA plans of ss-IMRT, d-IMRT, and VMAT target were -2.4%, -1.9%, and -1.1%, respectively.

The highest variation at the tumor-lung junction of these outcomes is shown in Table 1, regardless of delivery modalities or tumor volume. However, the largest variation recorded in PBA was +12.9%, whereas the MCA showed minimal deviation, which is less than -0.8%. Also, maximum deviation was computed by PBA for ss-IMRT, and MCA calculates mini-

Table 1: Dose variation utilizing Gafchromic film and several treatment planning system dose calculation algorithms for Left Lung central tumor (LCT).

Evaluation Points	Dose Difference Calculated vs. Measured in percentage					
	ss-IMRT		d-IMRT		VMAT	
	PBA	MCA	PBA	MCA	PBA	MCA
1	+12.9	-2.1	+12.5	-1.6	+12.5	-1.2
2	+10.8	-1.9	+9.1	-1.4	+10.5	-1.1
3	+10.5	-1.6	+9.8	-1.1	+11.6	-1.0
4	+11.6	-1.4	+10.5	-0.9	+10.2	-0.8
5	+11.8	-1.9	+9.6	-1.4	+11.7	-1.2
6	+11.2	-1.8	+9.5	-1.5	+12.4	-1.1
7	+11.5	-2.2	+10.8	-1.7	+11.8	-1.2
8	+11.9	-2.4	+11.5	-1.9	+11.6	-1.1

ss-IMRT: Step and Shoot Intensity-Modulated Radiation Therapy; d-IMRT: Dynamic Intensity-Modulated Radiation Therapy; VMAT: Volumetric Modulated Arc Therapy; PBA: Pencil Beam Algorithm; MCA: Monte Carlo Algorithm; +: Overestimation; -: Underestimation

mum deviation for VMAT. Percentage of dose variation between Gafchromic film and TPS dose calculation algorithms at different points (Point 1 to Point 8) for ss-IMRT, d-IMRT and VMAT techniques were shown in Figure 2.

At an isocentric dose plane, for PBA generated evaluation, the 2D gamma passing index rate for criteria 3%/3 mm was 94.9 to 96.2%, whereas it is found to be 92.2% to 94.5% for criteria 2%/2 mm.

The same evaluation done using MCA provided 97.3% to 98.7% for the criterion 3%/3 mm, and 95.3% to 95.6% for the criteria

2%/2 mm.

Table 2 demonstrates the gamma passing index rate utilizing PBA and MCA with different passing criteria for LCT. For the criterion of 3% and 3 mm, the evaluation of the 2D gamma passing index rate for the normal lung, with the film at a plane 3.5 cm from the tumor plane, was 96.1% to 97.3% for PBA and 98.2% to 98.6% for MCA plans (Figure 3).

Left Lung Peripheral Tumor (LPT)

The absolute dose along the central axis differences measured for 37.799 cc target

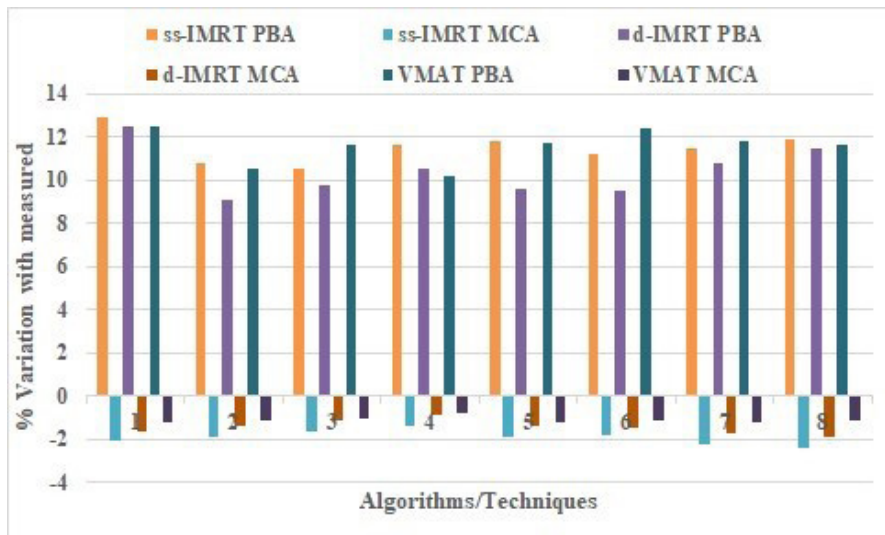


Figure 2: Techniques percentage dose variation between Gafchromic film and treatment planning system dose calculation algorithms at different points (Point 1 to Point 8).

Table 2: Percentage gamma passing index rate utilizing algorithms with varying passing criteria for left lung central tumor (LCT).

Evaluation Points	Dose Difference Calculated vs. Measured in percentage						
	ss-IMRT		d-IMRT		VMAT		
	PBA	MCA	PBA	MCA	PBA	MCA	
2D GPI at Iso-center	2%/2 mm	93.1	95.6	94.5	95.4	92.2	95.3
	3%/3 mm	95.3	97.3	96.2	98.7	94.9	97.5
	5%/5 mm	99.1	99.3	99.0	99.4	96.2	99.2
2D GPI at 3.5 cm	3%/3 mm	96.1	98.2	96.4	98.2	97.3	98.6

ss-IMRT: Step and Shoot Intensity-Modulated Radiation Therapy; D-IMRT: Dynamic Intensity-Modulated Radiation Therapy; VMAT: Volumetric Modulated Arc Therapy; PBA: Pencil Beam Algorithm; MCA: Monte Carlo Algorithm; GPI: Gamma Passing Index Rate

(LPT) computed using PBA plans of ss-IMRT, d-IMRT, and VMAT target were +13.0%, +12.5%, and +12.7%, respectively, for ss-IMRT, d-IMRT, and VMAT target; -2.6%, -2.1%, and -1.5% for MCA plans, accordingly.

Irrespective of delivery modalities or tumor volume, highest variation was found at the tumor-lung junction, as shown in Table 3. However, the largest variation was found in PBA (+13.0%), whereas the MCA showed minimal variation (<-1.5%). Also, the maximum variation was computed by PBA for ss-IMRT, and MCA calculated minimum deviation for VMAT, shown in Figure 4.

In an isocentric dose plane compared among PBA and measured, the 2D gamma passing index rate for criterion 3% with 3 mm was from 95.2% to 96.1%, whereas it was 92.1% to 92.4% for criteria 2 percent and 2 mm. The same comparison between MCA and measured yielded 96.6% and 97.5% for the criterion 3% and 3 mm, and 94.2% and 95.6% for the criteria 2%- and 2-mm. Table 4 demonstrates the gamma passing index rate utilizing PBA and MCA with different passing criteria for LPT.

For the criterion of 3% and 3 mm, the 2D Gamma assessment for the usual lung, with the film at the plane 3.5 cm from the tumor plane,

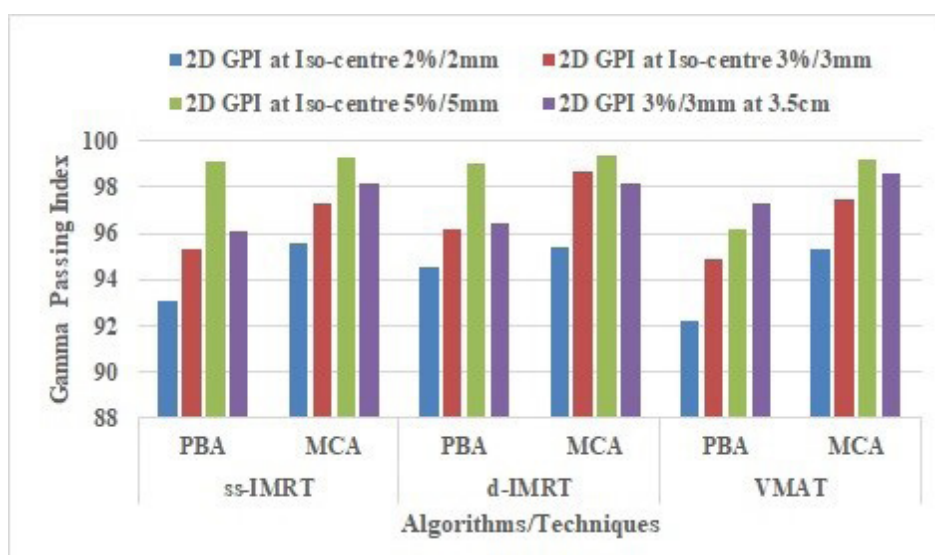


Figure 3: Algorithms/techniques gamma passing index variation between Gafchromic film fluence and treatment planning system dose fluence for left lung central tumor (LCT) with different passing criteria.

Table 3: Dose variation utilizing Gafchromic film and several treatment planning system dose calculation algorithms for left lung peripheral tumor (LPT)

Evaluation Points	Dose Difference Calculated vs. Measured in percentage					
	ss-IMRT		d-IMRT		VMAT	
	PBA	MCA	PBA	MCA	PBA	MCA
Peripheral Dose	+13.0	-2.6	+12.5	-2.1	+12.7	-1.5

ss-IMRT: Step and Shoot Intensity-Modulated Radiation Therapy; D-IMRT: Dynamic Intensity-Modulated Radiation Therapy; VMAT: Volumetric Modulated Arc Therapy; PBA: Pencil Beam Algorithm; MCA: Monte Carlo Algorithm; +: Overestimation; -: Underestimation

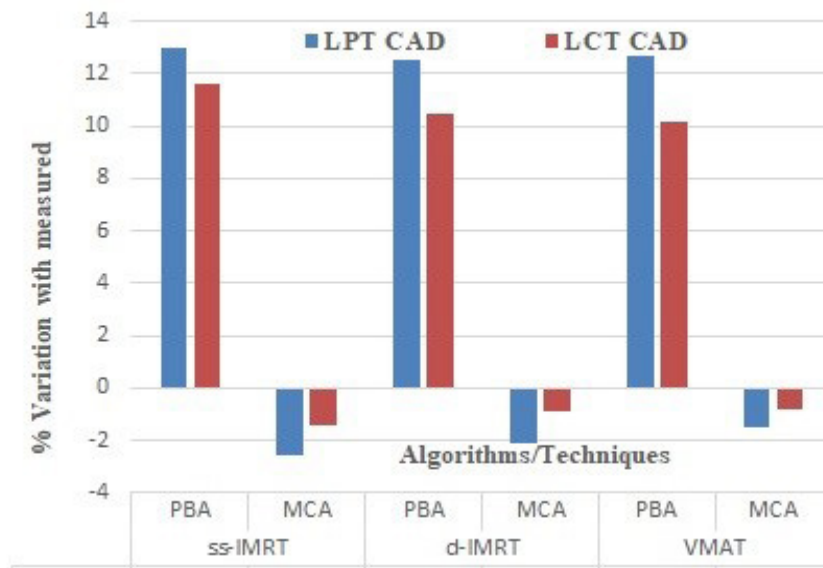


Figure 4: Techniques percentage dose variation between Gafchromic film and treatment planning system dose calculation algorithms at different points central axis dose (CAD) for left lung peripheral tumor (LPT) and left lung central tumor (LCT).

Table 4: Percentage Gamma Index passing rate utilizing Algorithms with varying passing criteria for Left lung peripheral tumor (LPT).

Evaluation Points	Dose Difference Calculated vs. Measured in percentage						
	ss-IMRT		d-IMRT		VMAT		
	PBA	MCA	PBA	MCA	PBA	MCA	
2D GPI at Iso-center	2%/2 mm	92.1	95.1	92.4	95.6	91.2	94.2
	3%/3 mm	95.2	96.6	96.1	97.5	95.2	96.7
	5%/5 mm	98.7	99.4	99.1	99.8	99.2	99.9
2D GPI at 3.5 cm	3%/3 mm	96.5	97.4	95.8	98.7	98.2	98.8

ss-IMRT: Step and Shoot Intensity-Modulated Radiation Therapy; D-IMRT: Dynamic Intensity-Modulated Radiation Therapy; VMAT: Volumetric Modulated Arc Therapy; PBA: Pencil Beam Algorithm; MCA: Monte Carlo Algorithm; GPI: Gamma Passing Index Rate

was 95.8% to 98.2% for PBA and 97.4% to 98.8% for MCA plans (Figure 5).

Discussion

In this study, EBT 3 Gafchromic film measured data for the lung heterogeneities when irradiated with a 6 MV photon beam to evaluate the dose calculation accuracy of two types of algorithms, PBA, and MCA. On the other

hand, previous evidence contrasted particular algorithms with theoretical Monte Carlo evidence or dose derived for a single tumor in the center of the lung alone [11, 16]. The authors of this study evaluated the reliability of algorithms with measurements taken at the central plane and the interface target of the lung. The difference is for the absolute dose at different points comprising tumor at the center and

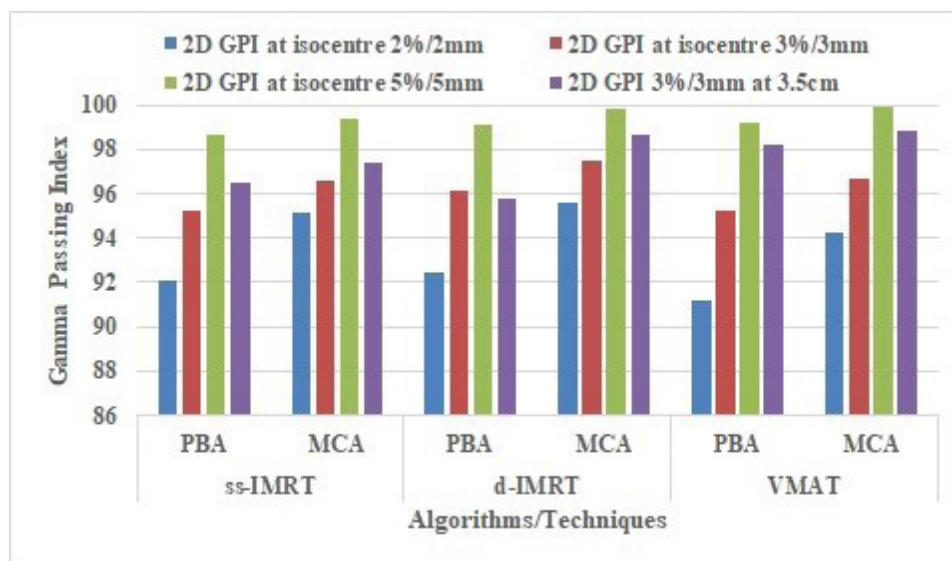


Figure 5: Algorithms/techniques gamma passing index variation between Gafchromic film fluence and treatment planning system dose fluence for left lung peripheral tumor (LPT) with different passing criteria.

interface of the lung, so the variation found could be slightly higher than in prior traditional Monte Carlo calculation.

In the present study, higher variations from measurement were reported for LCT with the PB algorithm across all points and tumor sizes. Even with the tough delta 2%/2 mm criterion, the 2D Gamma assessment passing rate is good for MCA, as shown in Tables 2 and 4.

Based on the evaluation of central axis points it reveals that the interface between the lung and the tumor is where algorithms fail most frequently. These discrepancies were as high as +13% in the PB algorithm against -1.5% in the MC algorithm, related to the capabilities of the algorithm in computing forward and transverse electronic disequilibrium, which is the primary reason for dose variation for the tumor. In dose plan evaluations, VMAT exhibits a high pass proportion and slight variation despite the algorithm. Also, the tumor at the interface has a relatively higher dose variation than the tumor center. The difference observed in the current study at the interface may be due to involvement, such as forward electronic dis-

equilibrium calculated by various algorithms. The findings of this study may incorporate statistical errors in the computations of commercialized algorithms, which may be reflected in the estimation of dose variation.

As more modulated and conformal therapeutic interventions become routine medical procedures, as in lung tumors, multi-institutional investigations of various dosimetric criteria should be employed to assess the efficacy of respective algorithms with the small fields, including heterogeneities present in adverse situations. Alagar AGB et al. [17] presented that maximum deviation among the algorithms was in the inter-face/junction of the lung and tumor. Similarly, in the current study, the same trend of results irrespective of treatment techniques was considered. In the present study, regardless of delivery mode, MC and PB algorithms exhibited the highest variation near the tumor-lung junction in both central and interfaced tumors. However, the variation with PBA was greater than MCA-generated VMAT plan, with a minimal permissible deviation of 0.8%, related to the lower accuracy of algorithm in

simulating the enhanced transverse scattering phenomenon in low-density mediums. Saini A et al. [18] showed that the greatest dose variation predicted by the PB method was -11.6% of the observed Gafchromic film dose in 15 MV photon energy. The maximal variation in dose was similarly large in all other energies. The largest dose variation predicted by the MC method was 2.04% of the observed Gafchromic film dose in 6 MVFFF photon energy. For all other energies (6 MV, 10 MV, and 15 MV and 6 MVFFF as well as 10 MVFFF), the dose variation was within 2%, which was consistent with dose variation of the current study. The Monte Carlo algorithm is reasonably precise with somewhat longer computational timeframes since it accounts for all physical phenomena, including inhomogeneity effects caused by scattered radiation, electron density, and electrons. For current findings, MC also performs Gafchromic film within tolerance limits. The efficacy of the MCA for LCT and LPT for ss-IMRT, d-IMRT, and VMAT techniques to effectively account was evaluated for inhomogeneity under simple geometric situations. Patient-specific Quality Assurance (QA) should be performed with lung phantoms instead of homogeneous density solid phantoms.

Conclusion

In this study, both algorithms exhibit slightly higher variations in left lung peripheral tumor than in left lung central tumor, regardless of treatment techniques. As a result, the dose assessment for the peripheral tumor should be done carefully. In addition, in both centralized and interfaced tumors, both algorithms exhibit the highest variations near the tumor-lung junction. However, with the PB algorithm, the variation is larger whilst there is a minimum permissible deviation with the MC algorithm-generated VMAT plans. This may be due to less accuracy of algorithms used to simulate elevated lateral scatter events in low-density substances. It is recommended that patient-

specific QA should be preferred in lung phantoms instead of homogeneous density solid phantoms in thorax cases, including lung radiotherapy with irrespective of delivery techniques.

Acknowledgment

The authors thank Dr Bharat Kumar and Mr Aashutosh Kumar Mishra for significant insight and guidance while writing the Manuscript.

Authors' Contribution

A. Mishra devised the concept and wrote the paper's introduction and core manuscript draught. At the same time, T. Raj Verma, AK. Srivastava, S. Prasad Mishra, KK. Mittal, and SK. Singh gathered data and relevant material with A. Mishra and assisted with the authoring of related works. A. Mishra carried out the approach implementation and experimental research. A. Mishra, T. Raj Verma, AK. Srivastava, and S. Prasad Mishra worked on the results and analysis. R. Pathak, S. Prasad Mishra, and T. Raj Verma checked and supervised the research. KK. Mittal rendered clinical assistance. All authors reviewed, edited, and approved the final version of the work.

Ethical Approval

There is no research involving human subjects and animal experiments on this topic. So, there is no need for ethical approval. However, this study is a part of research work that has already been approved by the university ethics committee-wide ethical clearance number 92/2020-21.

Conflict of Interest

None

References

1. Mesbahi A. The effect of electronic disequilibrium on the received dose by lung in small fields with photon beams: Measurements and Monte Carlo study. *Iran J Radiat Res.* 2008;6:70-6.
2. Verma T, Painuly NK, Mishra SP, Shajahan M,

- Singh N, Bhatt ML, et al. Performance Evaluation of Algorithms in Lung IMRT: A comparison of Monte Carlo, Pencil Beam, Superposition, Fast Superposition and Convolution Algorithms. *J Biomed Phys Eng.* 2016;**6**(3):127-38. PubMed PMID: 27853720. PubMed PMCID: PMC5106545.
3. Young ME, Kornelsen RO. Dose corrections for low-density tissue inhomogeneities and air channels for 10-MV x rays. *Med Phys.* 1983;**10**(4):450-5. doi: 10.1118/1.595392. PubMed PMID: 6888356.
 4. Klein EE, Morrison A, Purdy JA, Graham MV, Matthews J. A volumetric study of measurements and calculations of lung density corrections for 6 and 18 MV photons. *Int J Radiat Oncol Biol Phys.* 1997;**37**(5):1163-70. doi: 10.1016/s0360-3016(97)00110-7. PMID: 9169827.
 5. Svensson GK. Quality assurance in radiation therapy: physics efforts. *Int J Radiat Oncol Biol Phys.* 1984;**10**(Suppl 1):23-9. doi: 10.1016/0360-3016(84)90441-3. PubMed PMID: 6735791.
 6. Wambersie A. The role of the ICRU in quality assurance in radiation therapy. *Int J Radiat Oncol Biol Phys.* 1984;**10**(Suppl 1):81-6. doi: 10.1016/0360-3016(84)90454-1. PubMed PMID: 6429103.
 7. Golestani A, Houshyari M, Mostaar A, Jabbari Arfaie A. Evaluation of Dose Calculation Algorithms of Isogray Treatment Planning System Using Measurement in Heterogeneous Phantom. *Rep Radiother Oncol.* 2015;**2**(3):e5320. doi: 10.17795/rro-5320.
 8. Verma TR, Painuly NK, Mishra SP, Singh N, Bhatt MLB, Jamal N, Pant MC. Evaluation of dose calculation accuracy of various algorithms in lung equivalent inhomogeneity: Comparison of calculated data with Gafchromic film measured results. *J Cancer Res Ther.* 2017;**13**(6):1007-14. doi: 10.4103/0973-1482.168992. PubMed PMID: 29237967.
 9. Nalbant N, Kesen D, Hatice B. Pre-treatment dose verification of IMRT using gafchromic EBT3 film and 2D array. *J Nucl Med Radiat Ther.* 2014;**5**(2):1-6. doi: 10.4172/2155-9619.1000182.
 10. Casanova Borca V, Pasquino M, Russo G, Grosso P, Cante D, Sciacero P, et al. Dosimetric characterization and use of GAFCHROMIC EBT3 film for IMRT dose verification. *J Appl Clin Med Phys.* 2013;**14**(2):4111. doi: 10.1120/jacmp.v14i2.4111. PubMed PMID: 23470940. PubMed PMCID: PMC5714357.
 11. Wen N, Lu S, Kim J, Qin Y, Huang Y, Zhao B, Liu C, Chetty IJ. Precise film dosimetry for stereotactic radiosurgery and stereotactic body radiotherapy quality assurance using Gafchromic™ EBT3 films. *Radiat Oncol.* 2016;**11**(1):132. doi: 10.1186/s13014-016-0709-4. PubMed PMID: 27716323. PubMed PMCID: PMC5050597.
 12. Tillikainen L, Helminen H, Torsti T, Siljamäki S, Alakuijala J, Pyyry J, Ulmer W. A 3D pencil-beam-based superposition algorithm for photon dose calculation in heterogeneous media. *Phys Med Biol.* 2008;**53**(14):3821-39. doi: 10.1088/0031-9155/53/14/008. PubMed PMID: 18583728.
 13. Gagné IM, Zavgorodni S. Evaluation of the analytical anisotropic algorithm in an extreme water-lung interface phantom using Monte Carlo dose calculations. *J Appl Clin Med Phys.* 2006;**8**(1):33-46. doi: 10.1120/jacmp.v8i1.2324. PubMed PMID: 17592451. PubMed PMCID: PMC5722400.
 14. Bragg CM, Conway J. Dosimetric verification of the anisotropic analytical algorithm for radiotherapy treatment planning. *Radiother Oncol.* 2006;**81**(3):315-23. doi: 10.1016/j.radonc.2006.10.020. PubMed PMID: 17125862.
 15. Stathakis S, Esquivel C, Quino LV, Myers P, Calvo O, Mavroidis P, et al. Accuracy of the small field dosimetry using the Acuros XB dose calculation algorithm within and beyond heterogeneous media for 6 MV photon beams. *Int J Med Phys Clin Radiat Oncol.* 2012;**1**:78-87. doi: 10.4236/ijmp-cero.2012.13011.
 16. Ojala JJ, Kapanen MK, Hyödynmaa SJ, Wigren TK, Pitkänen MA. Performance of dose calculation algorithms from three generations in lung SBRT: comparison with full Monte Carlo-based dose distributions. *J Appl Clin Med Phys.* 2014;**15**(2):4662. doi: 10.1120/jacmp.v15i2.4662. PubMed PMID: 24710454. PubMed PMCID: PMC5875463.
 17. Alagar AGB, Ganesh KM, Kaviarasu K. Dose Calculation Accuracy of AAA and AcurosXB Algorithms for Small Central and Interface Lung Lesions - Verification with Gafchromic Film Dosimetry. *Asian Pac J Cancer Prev.* 2018;**19**(1):253-9. doi: 10.22034/APJCP.2018.19.1.253. PubMed PMID: 29374410. PubMed PMCID: PMC5844627.
 18. Saini A, Pandey VP, Singh A, Kumar P. Evaluating impact of medium variation on dose calculated through planning system in a low cost in-house phantom. *Biomed Phys Eng Express.* 2022;**8**(2):025022. doi: 10.1088/2057-1976/ac53bc. PubMed PMID: 35144251.